

Topology authentication for CAPD models based on laplacian coordinates

Abstract

The intellectual property protection for 3D CAPD (computer-aided plant design) models features their intrinsic complex topology relation. This paper discusses digital watermarking technology for 3D CAPD models defined by using parametric solids, which may offer a solution to topology authentication. We first analyze the geometrical and topological structures of CAPD models, followed by discussion on the topology protection problem. Then we propose an effective semi-fragile watermarking method for topology authentication based on Laplacian coordinates and quantization index modulation (QIM) against several attacks. We compute the custom Laplacian coordinate vector for each mark connection point according to the topological relation among the joint plant components. The content-based watermark for each mark connection point is generated from selected attributes of its joint plant component. Watermarks are inserted into the coordinates of mark connection points by adjusting the lengths of their Laplacian coordinate vectors. Experimental results demonstrate that our approach not only can detect and locate malicious topology attacks such as components modification and joint ends modification, but also is robust against various non-malicious attacks such as similarity transformations and level-of-detail(LOD).

Keywords: Semi-fragile watermarking, Fragile watermarking,

1. Introduction

2 Today's market is characterized by increasing competition. Companies
3 need to find ways and means of reducing project costs and diminishing re-
4 sources within basic and detail engineering, while at the same time sustaining
5 optimum productivity. And this calls for improvements in process plant de-
6 sign [1]. Process plants are complex facilities mainly consisting of various
7 plant components, such as equipments and pipelines which include pipes and
8 piping components. In order to facilitate process plant design processes, re-
9 search is actively carried out for developing methodologies and technologies
10 of collaborative computer-aided plant design (CAPD) systems to support
11 design teams geographically dispersed based on the quickly evolving infor-
12 mation technologies. The CAPD system is an automatic solution provided
13 for helping increase productivity, accuracy, and collaboration to meet the
14 challenges of complex plant design projects. And it often refers to the au-
15 tomation technologies, work practices and business rules supporting the engi-
16 neering and design of plants. In a collaborative CAPD system, designers and
17 engineers inevitably share their work with globally distributed colleagues.
18 Therefore, it is essential to confirm the integrity of all models for companies
19 when sharing models with their collaborators. Digital semi-fragile water-
20 marking provides a simple and reasonable solution for the integrity check of
21 CPAD models [2].

22 Generally, we can describe the CAPD model by three kinds of informa-
23 tion completely: the geometry information, the topology information and

24 the engineering information. The geometry information describes the shape
25 and 3D positions of all plant components. The topology information pro-
26 vides the complex topology relations among different plant components. The
27 engineering information refers to design constraints, engineering disciplines
28 and so on. Unlike the traditional mechanical computer aided design (CAD)
29 industry which mainly concentrates on the geometric modeling, the CAPD
30 systems mainly focuses on optimizing the plant layout[1]. Plant layout design
31 devotes to find the most economical spatial arrangement of process vessels
32 and equipment and their interconnecting pipes that satisfies construction,
33 operation, maintenance, and safety requirements[3]. This is an important
34 aspect in the design of process plants since a good layout will ensure that the
35 plant functions correctly and will provide an economically acceptable balance
36 between the many, often conflicting, design constraints [4]. Therefore, the
37 topology information protecting is a significant part of intellectual property
38 protection for CAPD models.

39 However, in the literature, existing watermarking schemes mainly target
40 traditional mechanical 2D CAD drawings or 3D CAD models. Furthermore,
41 these watermarking techniques mainly concentrate on the geometry informa-
42 tion protection. Thus topology protection for CAPD models is still in its
43 infancy and offers very interesting potentials for improvements because of
44 their intrinsic complex topology. In this paper, we propose a semi-fragile
45 watermarking scheme for addressing the issue of verifying the integrity of the
46 topology information for CAPD models. The topology information is tak-
47 en into consideration for both of the watermark generation and embedding.
48 And the content-based watermarks are embedded in a subset of the model's

49 connection points to keep them in a predefined relationship with neighboring
50 connection points so that any changes will ruin the relationship between the
51 marked connection points and neighboring connection points.

52 The rest of this paper is organized as follows. We review some related
53 works in Section 2. Section 3 gives a brief introduction of CAPD mod-
54 els. Section 4 describes the proposed scheme. Experimental results that
55 demonstrate our watermarking scheme performance are presented in Section
56 5. Conclusions follow in Section 6.

57 **2. Related work**

58 We review some related works about watermarking 3D CAD models in
59 this section.

60 Digital watermarking techniques for 3D models have been widely stud-
61 ied since Ohbuchi first proposed a watermarking scheme for 3D models[5].
62 However, relatively few watermarking algorithms have been proposed for 3D
63 CAD models especially for CAPD models. Watermarking schemes for 3D
64 CAD models mainly target CAD-based drawings, NURBS curves, subdivi-
65 sion surfaces, CSG models, etc..

66 A CAD drawing can be represented by various geometric objects in some
67 layers such as LINES, ARCS, POLYGONS and 3DFACEs, which include the
68 basic components of vertex, angle, radius, and so on. Park et al. proposed
69 a digital watermarking scheme for 3D CAD drawings [6]. The scheme uses
70 LINES and 3D FACEs based on vertex in CAD system to prevent infringe-
71 ment of copyright from unlawfulness reproductions and distribution. Kwon
72 et al. also proposed a watermarking scheme for 3D CAD drawings[7, 8]. The

73 approach arbitrarily selects the LINE, FACE, and ARC components and em-
74 beds the watermark into the difference in length between the reference line
75 and the connected lines in the case of line components, the circular radius
76 in the case of the arc components, and the length ratio of two sides in the
77 case of the face components. These schemes require the index and order
78 of embedding components and the original point coordinates for watermark
79 extraction. Therefore, they cannot detect watermarks when the components
80 of the drawing are rearranged. A robust watermarking scheme based on ge-
81 ometric features with k-means++ clustering for the 3D CAD drawings was
82 presented by Lee et al. [9]. The proposed scheme embeds the watermark
83 into the geometric distribution of POLYLINE, 3DFACE, and ARC objects
84 in the main layers. Ohbuchi et al. presented a watermarking scheme for 3D
85 NURBS curves using reparameterization [10]. Their method is robust under
86 affine transformations, but not under Möbius reparameterization. Lee et al.
87 also present a method for watermarking NURBS data using two-dimensional
88 virtual images[11]. A fragile watermarking schemes for authenticating CSG
89 models was proposed by Fornaro and Sanna [12]. It computes the watermark
90 from selected attributes of the model and stores it in one or more places
91 into the model itself. Weng et al. proposed a method for watermarking T-
92 spline curves and surfaces by using knot insertion[13]. In order to watermark
93 subdivision surfaces, Cheung et al. present a robust non-blind watermark-
94 ing scheme using modulating spectral coefficients of the subdivision control
95 mesh[14]. Reuter et al. introduced a method to extract Shape-DNA, a nu-
96 merical fingerprint or signature, of any 2d or 3d manifold (surface or solid) by
97 taking the eigenvalues (i.e. the spectrum) of its Laplace-Beltrami operator

98 [15]. It uses the sequence of eigenvalues (spectrum) of the Laplace operator
99 of a planar domain or 3d solid or the Laplace-Beltrami operator of a surface
100 or parameterized solid in Euclidean space as a fingerprint.

101 **3. CAPD Models**

102 We give a brief introduction of the geometrical and topological modeling
103 of CAPD models in this section.

104 *3.1. Geometrical modeling*

105 CAPD systems mainly focus on providing an effective and efficient plat-
106 form to concentrate on the layout of tremendous number of plant components
107 under complex constraints rather than shapes. Plant components are created
108 using CSG (Constructive Solid Geometry) representation by combining basic
109 solid entities which have simple shape such as sphere, cylinder, cone, etc..

110 In order to support the automatic generation of construction documents,
111 such as isometrics, orthographics, etc., which directly exchanged with the
112 model, plant components are defined using parameters. The main section-
113 s of a solid entity in the CAPD file are handle, entity type and geometric
114 parameters. An example of a sphere entity is shown in Fig. 1. Plant com-
115 ponents placed in a design model are parametric objects with a high degree
116 of intelligence. Designers progressively construct a highly intelligent design
117 database by placing instances of parametric components into the model.

118 *3.2. Topological modeling*

119 The layout poses significant limitations on the type, size and location of
120 plant components. Positions of plant components can be simply described

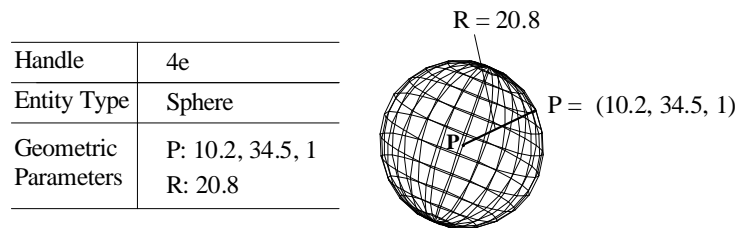


Figure 1: An example of a sphere entity.

121 by their absolute cartesian coordinates. But how to represent the intercon-
 122 nections among plant components is a key issue of CAPD systems. Not
 123 only should the layout represent the interconnection among two plant com-
 124 ponents, but it should also describe their interconnection ends. Only the two
 125 ends of different plant components which satisfy the specific requirements,
 126 such as pipe diameter, end type, pressure rating, and flow direction, can then
 127 be connected.

128 End connection can be mainly represented in two formats: connection
 129 points [16] and the order of plant components stored in the CAPD file. This
 130 paper aims to watermark CAPD models which describe the end connection
 131 by connection points since this format is one of the most widely used and
 132 effective representation for topological modeling.

133 Fig. 2 shows the main structure of connection points. Each connec-
 134 tion point has the same attributes including geometry information, topology
 135 constraint, handle value and various engineering properties. And each con-
 136 nection point may have one joint connection point at most. In general, a
 137 connection point is defined as the center point of the end face. And it is
 138 added, deleted and transformed along with its corresponding plant compo-
 139 nent in CAPD systems. Connection points can be classified into two kinds:

140 invariant connection points and variant connection points. Invariant con-
 141 nection points have just to do with the structure of their plant components.
 142 While variant connection points are concomitant with some operations. For
 143 example, a new connection point will be added at the joint when we inserting
 144 a nozzle to an equipment. Unlike pipes and piping components, the number
 145 of connection points of equipments may hold is unlimited in theory. Fig.
 146 3(a) shows connection points of some selected plant components. Fig. 3(b)
 147 shows the connection points of a simple pipeline. The interconnection be-
 148 tween the two joint plant components C_1 and C_2 is represented through their
 149 connection points $P_{1,1}$ and $P_{2,0}$ respectively.

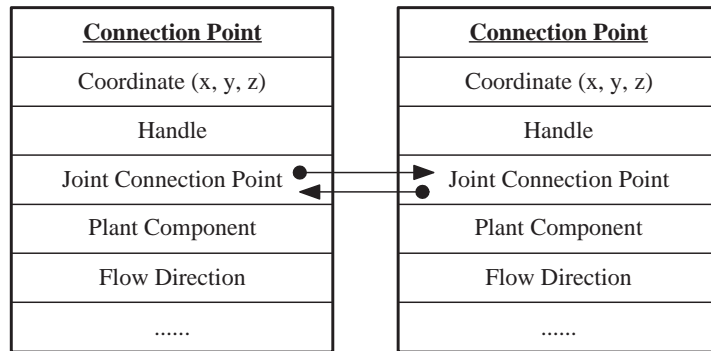


Figure 2: The structure of connection points.

150 In this paper, we discuss the problem of topology authentication for
 151 CAPD models from the following two aspects: joint plant components au-
 152 thentication and joint ends authentication. Joint plant components authen-
 153 tication aims to make sure that whether the joint plant components of each
 154 plant component are changed or not. While joint ends authentication further
 155 verifies whether the exact joint ends between the two joint plant components
 156 are modified or not. That is to say that, for each plant component, the

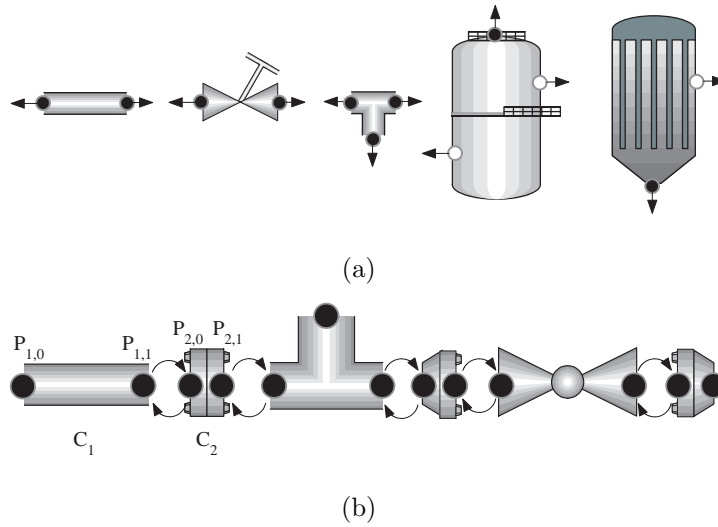


Figure 3: Examples of connection points of individual plant components and a simple pipeline. Black points are invariant connection points while white points are variant connection points. Note that all the connection points are scaled for better illustration. (a) Connection points of some selected plant components. (b) Connection points of a simple pipeline.

157 problem of topology authentication targets to verify not only its joint com-
 158 ponents, but also the exact joint ends, since a plant component usually has
 159 more than one joint ends.

160 4. The watermarking scheme for topology authentication

161 This section describes our topology verification method inspired on tra-
 162 ditional Laplacian operators.

163 4.1. Overview of the method

164 The proposed watermarking scheme consists of two separate procedures,
 165 the *embedding procedure* and the *extraction procedure*, which is shown in Fig.

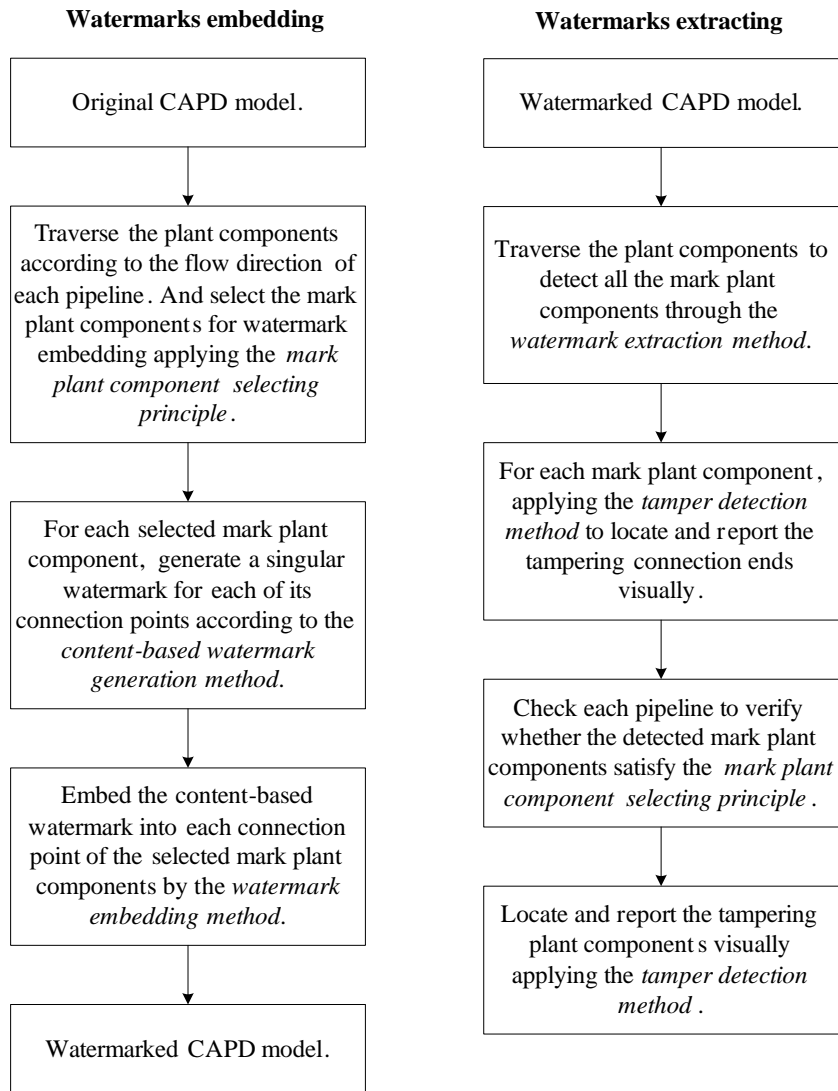


Figure 4: Overview of the proposed semi-fragile watermarking scheme.

166 4. The overview of the proposed watermarking scheme is described as follows.

167 In the watermark embedding stage, we first traverse the plant compo-
168 nents of each pipeline according to its flow direction and select the mark plant
169 components following the *mark component selecting principle*. Then, for each
170 selected mark plant components, we generate a singular content-based water-
171 mark for each of its connection points, which are also called mark connection
172 points, according to the *content-based watermark generation method*. After
173 that, we calculate the Laplacian coordinate vector through the *computa-*
174 *tion of laplacian coordinate method* for each mark connection point. Finally,
175 the content-based watermark is embedded into each mark connection point
176 through modifying the length of its Laplacian coordinate vector based on the
177 *watermarks embedding method*.

178 In the watermark extraction stage, the scheme uses the *watermarks ex-*
179 *tracting method* to detect and label all the mark plant components of the
180 watermarked model. For each mark plant component, we first extract the
181 embedded watermarks according to the *watermark extraction method* for
182 each of its connection points. Second, we use the *content-based watermark*
183 *generation method* to calculate the content-based watermarks for each of its
184 connection point. Third, we verify the topology integrity of each joint end
185 of the mark plant component by comparing the extracted watermarks with
186 the calculated content-based watermarks applying the *tempering detection*
187 *method*. Last, we report the tampering joint ends of the mark plant compo-
188 nent visually. For each pipeline, we verify whether the detected mark plant
189 components satisfy the *mark component selecting principle*. For those plant
190 components which do not meet the *mark component selecting principle*, we

191 locate and report them as suspicious tampering plant components visually.

192 4.2. Watermark targets

193 The objective of our scheme is to insert the watermark bits into the
194 model to verify not only the joint plant components, but also the exact
195 joint connection ends. To embed the watermark bits, a difficulty arise in our
196 case: the geometrical parameters of plant components should be kept unmodi-
197 fied. Otherwise, the modification will inevitably lead to generate construction
198 documents incorrectly. In other words, that means the watermarks should
199 not be embedded into the geometrical parameters of CAPD models.

200 To resolve this issue, we argue that the connection points are the best
201 candidates for data embedding because of the following reasons. First, the
202 topological relation among different plant components is described by their
203 connection points. Second, each end face of plant components has one and
204 only one associated connection point. And connection points are by definition
205 the least likely to be removed among the types of data objects that exist in
206 CAPD models. Moreover, the deletion of connection points will inevitably
207 lead to generate construction documents incorrectly.

208 4.3. Mark plant components selecting principle

209 We describe how to select the mark plant components in this section. We
210 initially set all plant components as *non-mark* components and traverse each
211 pipeline of the whole model to get eligible plant components for watermark
212 embedding according to the flow direction following the discipline below.

- 213 • One of the two joint plant components should be selected as a mark
214 plant component.

215 • The plant component chosen as a mark plant component must have
216 no mark components among its 1-ring neighboring components. Once
217 a plant component has been chosen as a mark component, its 1-ring
218 neighboring components are no longer eligible.

219 This principle is quite simple, and Fig. 5 shows two different selection
220 results for a same abstracted CAPD model. The union of the mark plant
221 components and their 1-ring neighborhood covers all the plant components of
222 the model. All the connection points of the selected mark plant components
223 are set as mark connection points and then used for watermark embedding.
224 Thus, it can be guaranteed that the mark plant components and their mark
225 connection points are uniformly distributed in the models. Experimental
226 data in Table 1 show that our principle selects around 50% of plant compo-
227 nents and connection points as mark plant components and mark connection
228 points respectively. And this can result in high locating accuracy which will
229 be discussed in Section 5.2.

230 4.4. Content-based watermark generation

231 We generate a content-based watermark for each mark connection point
232 taking some singular properties of its joint connection point and joint plant
233 component into consideration using a deterministic chaotic map.

234 Let C_m be a selected mark plant component with n connection points.
235 Plant component C_{m+1} is one of the joint plant components of C_m . $P_{m,i}$ is
236 a mark connection point of C_m ($i \in [0, n - 1]$). $P_{m+1,j}$ denotes a connection
237 point of C_{m+1} . Assume that the joint connection point of $P_{m,i}$ is $P_{m+1,j}$.
238 We denote the handle value of $P_{m+1,j}$ as $pHandle_{m+1,j}$. The handle value is

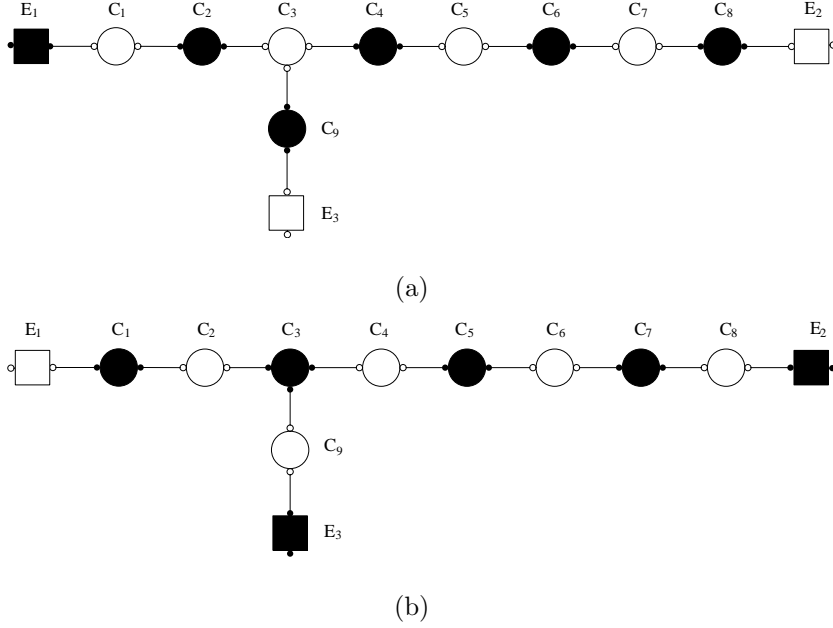


Figure 5: Two different selection results of mark plant components for a same simple abstracted CAPD model. The circular nodes represent pipe components while the rectangular nodes represent equipments. The black nodes are selected mark plant components while the white nodes are non-mark plant components.

239 involved in the construction of the watermarks, since each object in CAPD
 240 models has an unique handle value and it is not changed even if the object
 241 is modified[17]. Let the total number of joint plant components of C_{m+1} be
 242 d_{m+1} . And it is also involved in the watermark generation. The chaotic
 243 map used in this paper for the watermark generation is a well-known logistic
 244 function shown as follows:

$$f(x_n) = x_{n+1} = ax_n(1 - x_n), \quad (1)$$

245 where a is a positive number that acts as a function seed, and x_n is a number
 246 between 0 and 1, representing the current value of the mapping in time

247 with an initial value x_0 [18]. When $a > 3.5699456$, the sequence iterated
 248 with an initial value is chaotic. Different sequences will be generated with
 249 different initial values since the logistic function is extremely sensitive to
 250 initial conditions. The complicated but deterministic properties of the map
 251 make it ideally suited for watermark generation [19, 20, 21].

252 In order to generate the watermark $w_{m,i}$ for $P_{m,i}$, the handel value $pHandle_{m+1,j}$
 253 of $P_{m+1,j}$ is first converted into a positive float number $h_{m,i}$ ($0 < h_{m,i} < 1$)
 254 by

$$h_{m,i} = hash(pHandle_{m+1,j}), \quad (2)$$

255 where $hash()$ is a hash function. Then the logistic function, shown in Eq.1,
 256 is seeded with an initial starting value of $x_0 = h_{m,i}$, and iterated, and a final
 257 float value $f_{m,i}$ is calculated. After that we generate the watermark $w_{m,i}$
 258 ($0 < w_{m,i} < 1$) by

$$w_{m,i} = d_{m+1} \times f_{m,i}. \quad (3)$$

259 It should point out that there may be some mark connection points which
 260 have no joint connection points. In general, those selected mark plant com-
 261 ponents at the start or end position of a pipeline may have one or more mark
 262 connection points with no joint connection points. Take the mark plant com-
 263 ponent E_1 in Fig.5(a) for example, it has two mark connection points but
 264 only one of them has a joint connection point. We assume that $P_{m,i}$ has no
 265 joint connection point. And its handle is denoted as $pHandle_{m,i}$. Let the
 266 total number of joint plant components of C_m be d_m . In order to generate
 267 a watermark $w_{m,i}$ for $P_{m,i}$, then the positive number $h_{m,i}$ ($0 < h_{m,i} < 1$) for

268 $P_{m,i}$ is calculated by

$$h_{m,i} = \text{hash}(pHandle_{m,i}). \quad (4)$$

269 And the watermark $w_{m,i}$ ($0 < w_{m,i} < 1$) is finally generated by

$$w_{m,i} = d_m \times f_{m,i}. \quad (5)$$

270 4.5. The watermark embedding

271 In order to embed the watermark, we first calculate the Laplacian coor-
272 dinate vector δ for each mark connection point. Then we alert the Laplacian
273 length l , computing a new length \hat{l} carrying the watermark. Finally, the new
274 Laplacian vector $\hat{\delta}$ with length \hat{l} is realized through a minimization process,
275 and eventually the corresponding Cartesian coordinate is computed.

276 4.5.1. The computation of laplacian coordinates

277 For each connection point $P_{m,i}$ of C_m , we first define its neighboring con-
278 nection points using the following terminology: the neighboring connection
279 points $N(P_{m,i})$ is the set of all the connection points of the joint plant com-
280 ponents of $P_{m,i}$. $P_{m,i}$ is conventionally represented using absolute Cartesian
281 coordinates, denoted by $P_{m,i} = (x_{m,i}, y_{m,i}, z_{m,i})$. Fig. 6 shows an exam-
282 ple of the neighboring connection points of a mark connection point. The
283 mark component C_1 is a flange while its joint component C_2 is a valve.
284 $P_{1,1}$ is a mark connection point of C_1 . The neighboring connection points
285 $N(P_{1,1}) = \{P_{2,0}, P_{2,1}, P_{2,2}\}$, where $P_{2,0}$, $P_{2,1}$, and $P_{2,2}$ are connection points
286 of C_2 .

287 Then, we define the *differential* or δ - *coordinates* of $P_{m,i}$ to be the
288 difference between the absolute coordinates of $P_{m,i}$ and the center of mass of

289 the neighboring connection points of $P_{m,i}$,

$$\delta_{m,i} = (x'_{m,i}, y'_{m,i}, z'_{m,i}) = P_{m,i} - \frac{1}{d_{m,i}} \sum_{P_{m,j} \in N(P_{m,i})} P_{m,j} \quad (6)$$

290 where $d_{m,i} = |N(P_{m,i})|$ is the number of neighboring connection points of
 291 $P_{m,i}$. $\delta_{m,i}$ is also called the Laplacian coordinate of $P_{m,i}$. The length of
 292 the Laplacian coordinate vector is then selected as the watermark carrier for
 293 topology protection

$$l_{m,i} = \|\delta_{m,i}\| = \sqrt{(x'_{m,i})^2 + (y'_{m,i})^2 + (z'_{m,i})^2}. \quad (7)$$

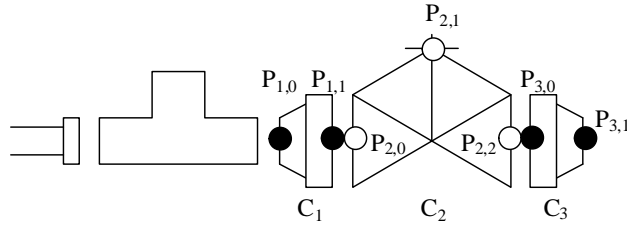


Figure 6: Illustration of the neighboring connection points of a mark connection point. C_1 is a flange and it is mark plant component while its joint component C_2 is a valve. The black point $P_{1,1}$ is a mark connection point of C_1 and its neighboring connection points are the white connection points $P_{2,0}$, $P_{2,1}$, and $P_{2,2}$ of C_2 .

294 As mentioned in Section 4.4, there may be some mark connection points
 295 with no joint plant components. For these mark connection points, we de-
 296 fine the connection points of the plant component they subject to as their
 297 neighboring connection points. For example, $P_{3,1}$ is a mark connection point
 298 of C_3 with no joint plant components in Fig.6. Its neighboring connection
 299 points $N(P_{3,1}) = \{P_{3,0}, P_{3,1}\}$, where $P_{3,0}$ and $P_{3,1}$ are all subject to C_3 .

300 4.5.2. *Quantization-based modulation*

301 After the calculation of Laplacian length, we describe our QIM based
302 watermark embedding method in this section.

303 We notice that the lengths of the Laplacian coordinates, unlike the Lapla-
304 cian coordinates themselves, are invariant under both translation and rota-
305 tion, but sensitive to uniform scaling. Therefore, two float factors S and f
306 are predefined as the keys for watermark embedding and extraction. The
307 initial value of S is set as the radius of the bounding sphere of the original
308 model. They are used to calculate the quantization step Δ ,

$$\Delta = \frac{R}{S} \times f, \quad (8)$$

309 where R is the radius of the bounding sphere of the model. It is obvious that
310 the quantization step Δ has a ratio to the radius of the bounding sphere of
311 the model. That is, a model with larger or smaller size will have larger or
312 smaller quantization step. Thus we can achieve uniform scaling invariance.

313 Fig. 7 illustrates how a watermark $w_{m,i}$ is embedded in the length $l_{m,i}$.
314 At first, we initialize the integer quotient $Q_{m,i}$ by $Q_{m,i} = \lfloor l_{m,i}/\Delta \rfloor$ with
315 the quantization step size Δ , where $\lfloor \cdot \rfloor$ represents the floor function. The
316 remainder $R_{m,i}$ is defined by $R_{m,i} = l_{m,i} - Q_{m,i} \times \Delta$. In general, $l_{m,i}$ cannot
317 be completely divided by Δ . In that case, the remainder R_i is discarded by
318 adjusting the the length $l_{m,i}$ such that $l_{m,i}^e$ can be divided by Δ

$$l_{m,i}^e = l_{m,i} - R_{m,i}. \quad (9)$$

319 Then we embed $w_{m,i}$ into $l_{m,i}$

$$\hat{l}_{m,i} = l_{m,i}^e + w_{m,i} \times \Delta \quad (10)$$

320 where $\hat{l}_{m,i}$ represent the length after embedding, $0 < w_{m,i} < 1$.

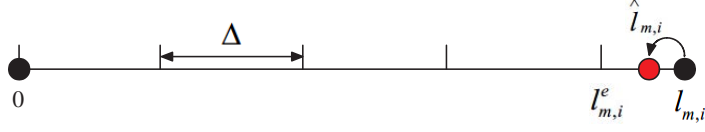


Figure 7: With the quantization step Δ , a watermark $w_{m,i}$ can be embedded by modifying the length $l_{m,i}$ to $\hat{l}_{m,i}$.

321 4.5.3. Distortion minimization

322 We discuss the calculation of the new Laplacian coordinate $\hat{\delta}_{m,i}$ after
 323 the computation of the embedded length $\hat{l}_{m,i}$ in this section. This is an
 324 undetermined problem and we solve it by minimizing the distance between
 325 the Laplacian coordinates before and after watermarking. We minimize the
 326 distance for each connection point by

$$(x'_{m,i} - x'_{\hat{m},i})^2 + (y'_{m,i} - y'_{\hat{m},i})^2 + (z'_{m,i} - z'_{\hat{m},i})^2 = \|\delta_{m,i} - \hat{\delta}_{m,i}\|^2 \quad (11)$$

327 subject to

$$(x'_{\hat{m},i})^2 + (y'_{\hat{m},i})^2 + (z'_{\hat{m},i})^2 = (\hat{l}_{m,i})^2 \quad (12)$$

328 This minimization problem is equivalent to finding a point $(x'_{\hat{m},i}, y'_{\hat{m},i}, z'_{\hat{m},i})$
 329 which is closest to the given point $(x'_{m,i}, y'_{m,i}, z'_{m,i})$ on a sphere C of radius
 330 $\hat{l}_{m,i}$ centered at the origin. We can take the point $(x'_{\hat{m},i}, y'_{\hat{m},i}, z'_{\hat{m},i})$ as the pro-
 331 jection of $(x'_{m,i}, y'_{m,i}, z'_{m,i})$ on C . As C is centered at the origin, the projection

332 of $(x'_{m,i}, y'_{m,i}, z'_{m,i})$ on it is given by

$$\left\{ \begin{array}{l}
 \hat{x}_{m,i} = \frac{x'_{m,i} l_{m,i}^{\hat{}}}{\sqrt{(x'_{m,i})^2 + (y'_{m,i})^2 + (z'_{m,i})^2}} \\
 \hat{y}_{m,i} = \frac{y'_{m,i} l_{m,i}^{\hat{}}}{\sqrt{(x'_{m,i})^2 + (y'_{m,i})^2 + (z'_{m,i})^2}} \\
 \hat{z}_{m,i} = \frac{z'_{m,i} l_{m,i}^{\hat{}}}{\sqrt{(x'_{m,i})^2 + (y'_{m,i})^2 + (z'_{m,i})^2}}
 \end{array} \right. \quad (13)$$

333 Finally, the Cartesian coordinate of the watermarked connection point
 334 can be computed from its Laplacian coordinate $(\hat{x}_{m,i}, \hat{y}_{m,i}, \hat{z}_{m,i})$ according to
 335 Eq. 6.

336 In our scheme, the distortion induced by watermark embedding depends
 337 on the quantization step Δ . From the Eq. 8, we can see that the larger
 338 the key value f , the larger the induced distortion, since the key value S is
 339 set to the radius R of the bounding sphere of the original model initially.
 340 Therefore, the maximum distortion from each mark connection point can be
 341 controlled by setting the key value f according to the precision requirement.

342 4.6. The watermark extraction and tamper detection

343 In the watermark extraction stage, we initially set all plant components
 344 and connection points as mark plant components and mark connection points
 345 respectively. S and f are the keys for malicious-change detection. And they
 346 are employed to calculate the quantization step Δ with Eq. 8. We first
 347 check and find out all of the mark plant components of the model. Then we
 348 apply the *mark plant components selecting principle* to detect and locate the
 349 tampered regions.

350 For each plant component C_m with n connection points, we check each
351 of its connection points $P_{m,i}$ ($0 \leq i \leq n - 1$) to see whether it is a mark
352 connection point or not. We first compute the length $l_{m,i}$ of the Laplacian
353 coordinate vector of $P_{m,i}$ with Eq.6 and Eq. 7. Then we extract the embedded
354 watermark with the quantization step Δ by

$$w'_{m,i} = \frac{(l_{m,i} - \lfloor \frac{l_{m,i}}{\Delta} \rfloor \times \Delta)}{\Delta} \quad (14)$$

355 In order to see whether $P_{m,i}$ is a mark connection point, the content-based
356 watermark $w_{m,i}$ for $P_{m,i}$ is generated according to the *content-based water-*
357 *mark generation method* described in Section 4.4. Thus, $w_{m,i}$ and $w'_{m,i}$ should
358 satisfy $w_{m,i} = w'_{m,i}$ if $P_{m,i}$ is a mark connection point. We label C_m as a mark
359 plant component if it has at least one mark connection point. Otherwise, C_m
360 is set to be a non-mark plant component.

361 After the labeling of mark connection points and mark plant components,
362 we next detect and locate the tampered plant components and connection
363 points applying the *mark plant components selecting principle*. For each
364 mark plant component, we set it as an unmodified plant component only
365 if all of its connection points are mark connection points. Otherwise, we
366 label its non-mark connection points and their joint plant components as
367 suspicious regions. For each pipeline of the model, we traverse its plant
368 components according to its flow direction and check if the labeled mark
369 plant components satisfy the *mark plant components selecting principle*. We
370 set those plant components which do not meet the *mark plant components*
371 *selecting principle* as tampered plant components.

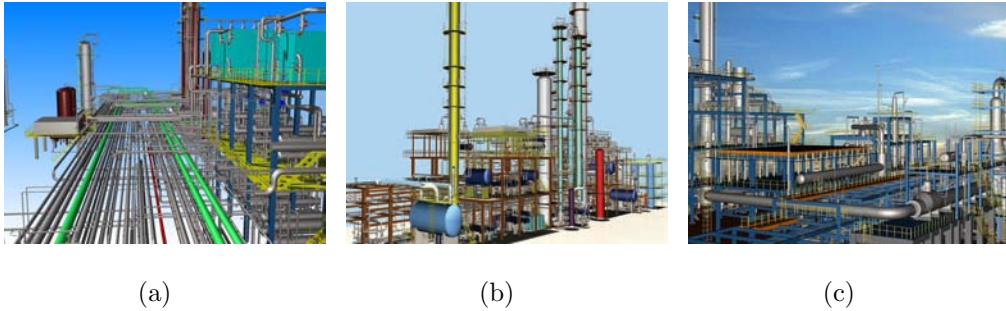


Figure 8: Three CAPD models used for experiments. (a)Carton board plant; (b)Hydrogenation plant; (c)Styrene plant.

372 5. Experimental results and discussion

373 To validate the feasibility of our topology verification algorithm, we first
 374 give some experimental results and then discuss its performance later in this
 375 section.

376 5.1. Experimental results

377 We evaluated the proposed semi-fragile watermarking scheme on a set
 378 of 3D CAPD models with various unauthorized attacks and three of them
 379 are shown in Fig. 8. Table 1 lists the detailed information about the three
 380 models. The following parameter settings are used in our experiments. The
 381 logistic function used for the watermark generation is seeded with a value
 382 $a = 4$ for 5000 iterations. The key value f is set to 10^{-3} according to the
 383 model precision and S is equal to the radius of the bounding sphere of each
 384 model listed in Table 1.

385 From Table 1 we can find that our approach selects around 50% of the
 386 plant components as mark plant components. And the watermark bits are
 387 embedded into nearly 50% of the connection points.

Table 1: Lists of three CAPD models used in our experiments and their detail information including plant components(PCs), connection points(CPs), mark plant components(MPCs), mark connection points(MCPs) and radius.

Model	PCs	CPs	MPCs	MCPs	Radius(m)
Carton board	6810	13964	3365	7002	118.890
Hydrogenation	15570	32624	8145	16556	104.380
Styrene	18912	38198	9652	19484	86.321

388 *5.1.1. Tamper detection and localization evaluation*

389 Fig. 9(a) and Fig. 9 (c) show a close view of part of the original hydro-
390 generation plant model rendered in solid and wireframe mode respectively. The
391 hydrogenation plant model has 15570 plant components and about 52.3% of
392 them are selected as mark plant components. Fig. 9(b) and Fig. 9(d) are the
393 same view of part of the watermarked model rendered in solid and wireframe
394 mode respectively, which are visually identical with the original model.

395 Fig. 10 illustrates that our scheme accurately detects and locates several
396 kinds of attacks simultaneously on a hydrogenation plant model. Fig. 10(a),
397 Fig. 10(c), Fig. 10(e) and Fig. 10(g) show a close view of the regions of
398 the watermarked hydrogenation plant model before being attacked illegally
399 by joint components modification and joint ends modification respectively.
400 The regions labeled A, B, C, and D denote the regions of joint components
401 addition, joint components deletion, disconnecting the two joint ends geomet-
402 rically and changing the topology relation between two joint ends logically,
403 respectively. Our scheme locates these changed regions by setting all detect-
404 ed suspicious plant components as suspicious regions. Fig. 10(b), Fig. 10(d),
405 Fig. 10(f) and Fig. 10(h) illustrate the located suspicious plant components

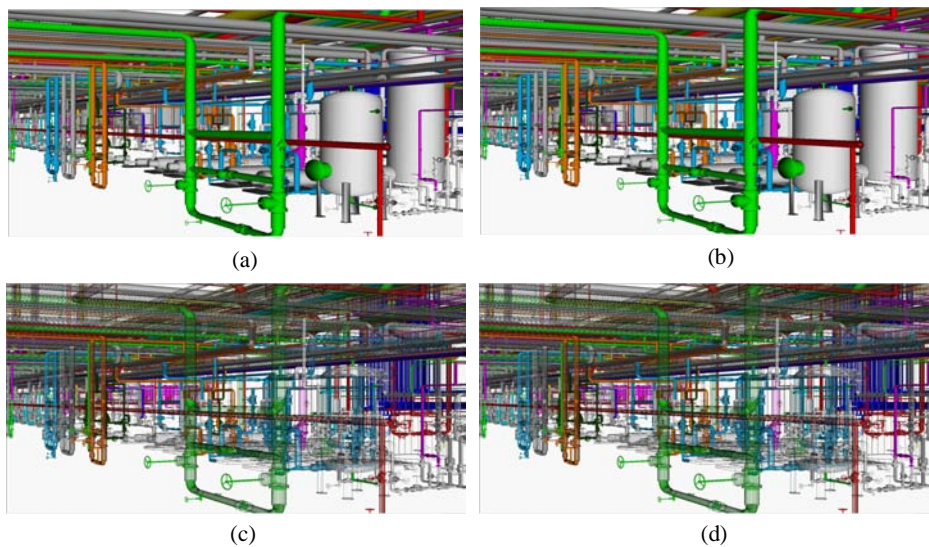


Figure 9: One example of semi-fragile watermarking. (a)(c) A close view of part of the original model rendered in solid and wireframe mode respectively. (b)(d) A close view of part of the watermarked model rendered in solid and wireframe mode respectively.

406 in red. From Fig. 10(b), Fig. 10(d), Fig. 10(f) and Fig. 10(h) we can find
 407 that the regions in red are exactly where the tampering operations happen.
 408 The experimental results verify the accuracy of our locating procedure.

409 5.1.2. Robustness evaluation

410 We evaluated the robustness against various operations provided by CAPD
 411 systems that can be considered to be non-malicious attacks on the design
 412 model. These non-malicious attacks include rotating, uniform scaling, trans-
 413 formation and LOD. The robustness of our semi-fragile watermarking scheme
 414 is evaluated in terms of the *BER* (bit error rate) of the extracted watermark
 415 bit sequence, as well as the correlation coefficient *Corr* between the extracted
 416 binary sequence $\{w_i^e\}$ and the originally embedded one $\{w_i^o\}$ as given by the

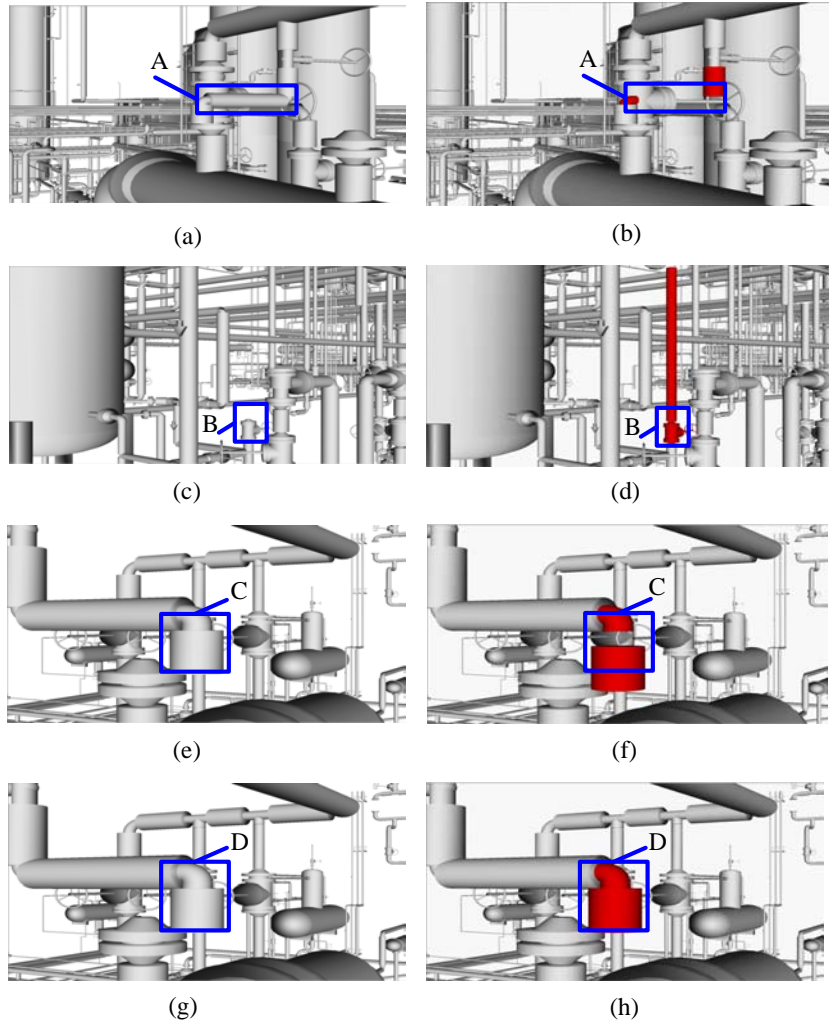


Figure 10: The proposed scheme works on a hydrogenation plant model.(a)(c)(e)(g) The regions before being attacked. Label A denotes the regions of joint components deletion. Label B denotes the regions of joint components addition. Label C denotes the regions of disconnecting the two joint ends geometrically, and label D denotes the region of changing the topology relation between two joint ends logically. (b)(d)(f)(h) Our scheme accurately locates these attacks visually.

Table 2: N_m/N_c of the three CAPD models after various non-malicious attacks.

Attacks	Carton board	Hydrogenation	Styrene
RST	0	0	0
LOD			
(80% triangles)	0	0	0
(60% triangles)	0	0	0
(40% triangles)	0	0	0

417 following equation [22]:

$$Corr = \frac{\sum_{i=0}^{n-1} (w_i^e - \overline{w^s})(w_i^o - \overline{w^o})}{\sqrt{\sum_{i=0}^{n-1} (w_i^e - \overline{w^s})^2} \times \sqrt{\sum_{i=0}^{n-1} (w_i^o - \overline{w^o})^2}}, \quad (15)$$

418 where $\overline{w^e}$ and $\overline{w^o}$ are, respectively, the averages of the watermark bit
419 sequence $\{w_i^e\}$ and $\{w_i^o\}$.

420 For each plant component, if the values of BER and $Corr$ are, respective-
421 ly, 0 and 1, then we can set the plant component as untampered. Otherwise
422 the plant component is detected as tampered. Let N_c be the total number
423 of plant components in a model and N_m be the number of plant components
424 detected as tampered. Table 2 presents the N_m/N_c of the three models after
425 various non-malicious attacks. And we can find that our scheme is robust
426 against these non-malicious operations.

427 5.1.3. Imperceptibility evaluation

428 For evaluating the subject imperceptibility, we compare the original hy-
429 drogenation plant model and the watermarked hydrogenation plant model

430 rendered in solid and wireframe mode respectively. Fig. 9 shows a close view
 431 of part of the original and watermarked hydrogenation plant model. And we
 432 can see the imperceptibility of the watermarked connection points.

433 In order to measure the objective distortion of the watermarked CAPD
 434 models induced by watermarking, we use the Metro [23] in terms of maxi-
 435 mum root mean square error(MRMS) for plant components and PSNR (peak
 436 signal-to-noise ratio) [9] for connection points respectively.

$$PSNR = 10 \lg \frac{MAX^2}{MSE}, \quad (16)$$

437 where

$$MAX = \max \|P_i - o\|, i \in [0, N - 1],$$

$$MSE = \frac{1}{N} \sum_{i=0}^{N-1} \|P_i - P'_i\|,$$

440 P_i and P'_i are the corresponding connection points in the original and wa-
 441 termarked model respectively, o is the geometric center of the model, N is
 442 the number of connection points, $\|P_i - P'_i\|$ is the Euclidean distance be-
 443 tween these two connection points. Table 3 lists the MRMS values of plant
 444 components and the PSNR values of connection points.

445 From the Table 3, we can see that the MRMS values are all 0, since
 446 our scheme prefers the connection points, which are integral parts of CAPD
 447 models, instead of the geometric parameters of plant components themselves
 448 as watermark carriers. That means we need not modify the geometric pa-
 449 rameters of plant components. Therefore our scheme has no influence on the
 450 geometry shape of CAPD models.

451 Although the connection points, compared with the large scale plant com-
 452 ponents, are nearly not seen by viewers because of their small size and little

Table 3: The MRMS values of plant components and PSNR values of connection points between the original and watermarked models.

Model	MRMS	PSNR(dB)
Carton board	0	68.56
Hydrogenation	0	81.03
Styrene	0	79.64

453 contribution to the final scene even rendered in wireframe mode, we still give
454 the PSNR values of connection points here. The impact of watermark em-
455 bedding on connection points could be tuned by the quantization step size
456 Δ . According to our *watermark embedding method* described in Section 4.5,
457 our scheme just slightly adjust the positions of mark connection points. And
458 the topology relation will not be alerted too. As a consequence, our scheme
459 will have no influence on the design and automatic generation of various
460 construction documents. Thus, our scheme is functionally imperceptible.

461 5.2. Discussion on tamper detection and localization

462 We analysis the performance of our scheme on detecting and locating the
463 tampered regions on the model from the following two aspects: attacks a-
464 gainst plant components and attacks against joint ends, both of which are
465 common operations in practical design process. Components attacks mainly
466 include adding, deleting and replacing plant components. While joint ends
467 attacks mainly include separating the two joint ends geometrically, discon-
468 necting the two joint ends logically and replacing the joint end.

469 5.2.1. *Components modification*

470 • **Components addition.** Without loss of generality, there mainly exist
471 three situations when adding plant components into the model which
472 is shown in Fig. 11. Plant components are represented by rectangular
473 nodes. The black nodes are mark plant components and their con-
474 nection points are watermarked. The white nodes are non-mark plant
475 components. The plant components to be added are represented by
476 red nodes.

477 First, Fig. 11(a) shows that a new plant component A_1 is added and it
478 is connected with an existing non-mark plant component C_1 . This kind
479 of attacks modifies the topological relation of C_1 . And it changes the
480 total number of joint plant components of C_1 from one to two. During
481 the watermark extraction stage, $P_{2,1}$ is labeled as a mark connection
482 point. Then C_2 is set as a mark plant component. However, the wa-
483 termark for $P_{2,0}$ generated according to the *content-based watermark*
484 *generation method* is different from the extracted original embedded
485 one. Thus the topological modification of C_1 , as well as $P_{2,0}$, is detect-
486 ed.

487 Second, Fig. 11(b) shows that a new plant component A_1 is added
488 and it is connected with an existing mark plant component C_2 . Thus
489 A_1 becomes the joint plant component of $P_{2,1}$. During the watermark
490 extraction stage, $P_{2,0}$ is labeled as a mark connection point. Then
491 C_2 is set as a mark plant component. But the watermark for $P_{2,1}$
492 generated according to the *content-based watermark generation method*
493 is different from the extracted original embedded one. Therefore the

494
495
496
497
498
499
500
501
502
503
504
505
506
507

topological modification of C_2 , as well as $P_{2,1}$, is detected.

Third, Fig. 11(c) shows that two new plant components A_1 and A_2 are added, and A_1 is inserted between the non-mark plant component C_1 and the mark plant component C_2 while A_2 is inserted between the non-mark plant component C_3 and the mark plant component C_2 . These attacks modify the topological relation of C_1 , C_2 and C_3 . During the watermark extraction stage, all the connection points are labeled as non-mark connection points according to the *watermark extraction and tamper detection method*. And then all the plant components are set as non-mark plant components. As a result, all the plant components are labeled as tampered plant components since they do not satisfy the *mark plant components selecting principle*. And Subsequently the topological modification of C_1 , C_2 and C_3 are detected and located accurately.

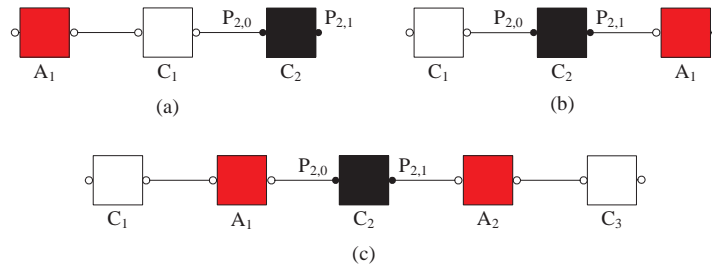


Figure 11: Illustration of detecting and localizing components addition. The black nodes are mark plant components. The white nodes are non-mark plant components. The red nodes represent the added plant components.

508
509

- **Components deletion.** These attacks modify the topological relation of the model. There are two main situations when deleting plant

510 components from the model shown in Fig.12: mark plant components
511 deletion and non-mark plant components deletion.

512 In Fig.12(a), a mark plant component D_1 is deleted. Thus the total
513 number of joint plant components of C_2 changes from two to one. C_1
514 is set as a mark plant component since $P_{1,0}$ is labeled as a mark con-
515 nection point during the watermark verification stage. The generated
516 watermark for $P_{1,1}$ is different from the extracted original one accord-
517 ing to the *content-based watermark generation method*. As a result, the
518 topological modification of C_2 is detected and located accurately.

519 In Fig.12(b), a non-mark plant component D_1 is deleted. Thus no
520 joint plant component is assigned to the mark connection point $P_{2,1}$.
521 C_2 is set as a mark plant component because $P_{2,0}$ is labeled as a mark
522 connection point during the watermark verification stage. However, the
523 generated watermark for $P_{2,1}$ is different from the extracted original
524 one according to the *content-based watermark generation method*. As
525 a result, the topological modification of C_2 , as well as $P_{2,1}$, induced by
526 components deletion is detected and located accurately.

527 • **Components replacing.** Two main situations arise when replacing
528 plant components from the model: replacing mark plant components
529 and replacing non-mark plant components.

530 In Fig.13(a), a mark plant component C_3 is replaced with a plant com-
531 ponent R . During the watermarking extraction stage, C_1 is labeled as
532 a mark plant component. However, the extracted watermarks from R
533 inevitably do not match the original embedded ones since the coordi-

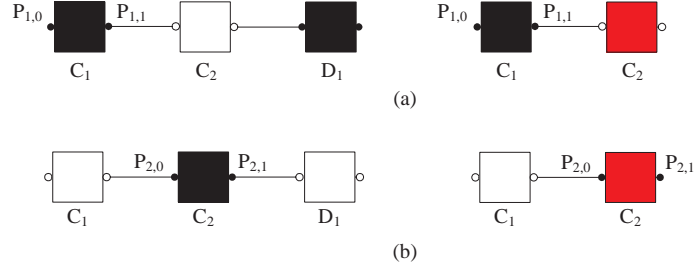


Figure 12: Illustration of detecting and localizing component deletion. The black nodes are mark plant components. The white nodes are non-mark plant components. The suspicious plant components are represented by red nodes.

534 nates of the connection points of R are different from the coordinates
 535 of the watermarked connection points of C_3 . And thus it is labeled as a
 536 non-mark plant component. As a result, R and C_2 are set as suspicious
 537 plant components since both of them are non-mark plant components
 538 applying *the mark plant components selecting principle*.

539 In Fig.13(a), a non-mark plant component C_3 is replaced with a plant
 540 component R . During the watermarking extraction stage, C_2 is labeled
 541 as a mark plant component since $P_{2,0}$ is set as a mark connection point.
 542 The generated watermark for $P_{2,1}$ is different from the extracted origi-
 543 nal one because the handle value of R is different from the handle
 544 value of C_3 . Hence the modification of the topological relation between
 545 $P_{2,1}$ and R induced by components replacing is detected and located
 546 accurately.

547 Note that we just take the same kind of plant components into consid-
 548 eration, since different kind of plant components may not only induce
 549 different handle values and coordinates but also induce different number

550 of connection points. These attacks can be detected relatively easily.

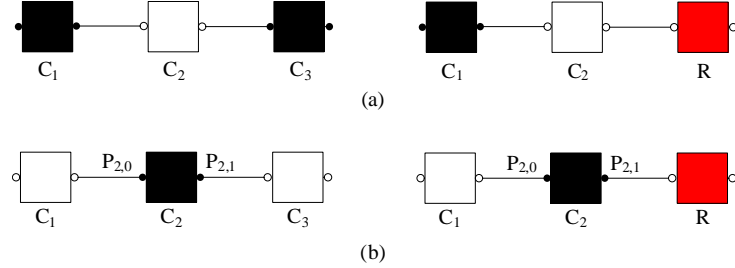


Figure 13: Illustration of detecting and localizing component replacing. The black nodes are mark plant components. The white nodes are non-mark plant components. The red nodes represent the plant components after replacing.

551 5.2.2. Joint ends modification

552 We discuss the attacks on the two joint connection ends in this section.
 553 These two attacked connection ends subject to two different joint plant com-
 554 ponents. And one should be a mark connection point while the other should
 555 be a non-mark connection point according to the *mark plant components*
 556 *selecting principle*.

- 557 • **Disconnect the two joint ends geometrically.** This kind of at-
 558 tacks separates one connection end from the other connection end ge-
 559 ometrically while keeps their topology relation logically. During the
 560 watermark extraction stage, the generated watermark for the attacked
 561 mark connection point is identical to the original embedded one since
 562 non topological modification is induced. However, the Laplacian coor-
 563 dinate vector of the attacked mark connection point is different from
 564 the original one because of the geometrical modification of the two at-
 565 tacked joint plant components. Therefore, the extracted watermark

566 is not match the original embedded one. As a result, the attacked
567 connection end and its joint plant component are detected.

568 • **Change the topology relation between two joint ends logically.**

569 This kind of topology attacks changes the topological relation between
570 the two joint ends logically. Thus the joint connection point of the mark
571 connection point is alerted. This modification leads to the difference
572 between the embedded watermark and the calculated watermark during
573 the watermark extraction stage. Consequently, the attacked two joint
574 ends are detected.

575 *5.3. Discussion on robustness against non-malicious attacks*

576 A good semi-fragile watermarking scheme should be invariant to trans-
577 lation, rotation, uniform scaling and LOD operations. These operations do
578 not change the integrity of the original model and should not be regarded as
579 malicious attacks.

580 *5.3.1. Robustness against similarity transformation*

581 These similarity transforming operations modify the coordinates of the
582 model. Our scheme prefers the lengths of the Laplacian coordinates to the
583 Laplacian coordinates themselves of the mark connection points as water-
584 mark carriers. Thus it is invariant under both translation and rotation. In
585 order to resist the uniform scaling operation, the radius of the bounding
586 sphere of the model is involved in the *quantization-based modulation* stage
587 for watermark embedding. That is, a model with larger or smaller size will
588 have larger or smaller quantization steps. Thus we can achieve uniform scal-
589 ing invariance.

590 5.3.2. *Robustness against level-of-detail*

591 For the past several years, the widespread use of collaborative CAPD
592 systems and the reuse of existing CAPD data in new designs have created
593 a data explosion in many application areas. And this has resulted in large
594 databases of complex CAPD models. As the complexity of CAPD model-
595 s increases, the enormous size of these CAD data sets poses a number of
596 challenges in terms of interactive display and manipulation. Thus, CAPD
597 systems must employ methods for filtering out as efficiently as possible the
598 data that isn't contributing to a particular image. LOD is a key technology
599 to reduce the model complexity and improve the rendering performance for
600 large scale complex CAPD models. A LOD model is a compact description of
601 multiple representations of a single shape and is the key element for provid-
602 ing the necessary degrees of freedom to achieve runtime adaptivity. However,
603 connection points and topological relation among plant components will not
604 be influenced by LOD since it can only change the details of entity sur-
605 faces. Therefore, the 1-ring neighboring points set of each mark connection
606 point will not be affected. Subsequently it will not change the centroid of
607 the neighborhood of mark points. As a result, our scheme is robust against
608 LOD.

609 **6. Conclusion**

610 This paper presents digital watermarking as a possible topology authenti-
611 cation tool to provide security to 3D CAPD models. Both of the topological
612 relation and singular attributes of plant components are taken into consid-
613 eration for the watermark generation and embedding. The watermarks are

614 embedded into the coordinates of mark connection points by adjusting the
615 lengths of their Laplacian coordinate vectors. Theoretical analysis and ex-
616 perimental results show that our semi-fragile scheme has a strong ability to
617 detect and locate malicious attacks which are common operations in practical
618 design process. Meanwhile, our scheme can exactly preserve the geometric
619 shape of plant components and hence has no effect on the automatic gener-
620 ation of construction documents.

621 [1] Burdorf A, Kampczyk B, Lederhose M, Schmidt-Traub H. Capd-
622 computer-aided plant design. *Computers and Chemical Engineering*
623 2004;28(1-2):73–81.

624 [2] Wang K, Lavoué G, Denis F, Baskurt A. A comprehensive survey on
625 three-dimensional mesh watermarking. *IEEE Transactions on Multime-
626 dia* 2008;10(8):1513–27.

627 [3] Guirardello R, Swaney R. Optimization of process plant layout with
628 pipe routing. *Computers & Chemical Engineering* 2005;30(1):99–114.

629 [4] Georgiadisa M, Macchietto S. Layout of process plants: A novel
630 approach. *Computers & Chemical Engineering* 1997;21(Supplement
631 1):S337–42.

632 [5] Ohbuchi R, Masuda H, Aono M. Watermarking three-dimensional
633 polygonal models. In: *Proceedings of the ACM Multimed.* Seattle,
634 USA; 1997, p. 261–72.

635 [6] Park HK, Lee SH, Kwon KR. Blind watermarking for copyright protec-
636 tion of 3d cad drawing. In: *Proceedings of the 8th International Con-*

- 637 ference on Advanced Communication Technology. Gangwon-Do, Korea;
638 2006, p. 253–6.
- 639 [7] Kwon K, Lee S, Lee E, Kwon S. Watermarking for 3d cad draw-
640 ings based on three components. Lecture Notes in Computer Science
641 2006;4109:217–25.
- 642 [8] Kwon K, Chang H, Jung GS, Moon K, Lee S. 3d cad drawing wa-
643 termarking based on three components. In: Proceedings of the IEEE
644 International Conference on Image Processing. Atlanta, GA, USA; 2006,
645 p. 1385–8.
- 646 [9] Lee SH, Kwon KR. Cad drawing watermarking scheme. Digital Signal
647 Processing 2010;20(5):1379–99.
- 648 [10] Ohbuchi R, Masuda H, Aono M. A shape-preserving data embedding al-
649 gorithm for nurbs curves and surfaces. In: Proceedings of the Computer
650 Graphics International. Alberta, Canada; 1999, p. 180–7.
- 651 [11] Lee JJ, Cho NI, Lee SU. Watermarking algorithms for 3d nurb-
652 s graphic data. EURASIP Journal on Applied Signal Processing
653 2004;2004(14):2142–52.
- 654 [12] Fornaro C, Sanna A. Public key watermarking for authentication of csg
655 models. Computer-Aided Design 2000;32(12):727–35.
- 656 [13] Weng B, Ri J, Yao Z, Yang S, Feng X, Pan. Z. Watermarking t-spline
657 surfaces. In: Proceedings of the 11th IEEE international conference
658 on communication technology proceedings. HangZhou, China; 2008, p.
659 773–6.

- 660 [14] Cheung YM, Wu HT. A sequential quantization strategy for data em-
661 bedding and integrity verification. *IEEE Transactions on Circuits and*
662 *Systems for Video Technology* 2007;17(8):1007–16.
- 663 [15] Reuter M, Wolter FE, Peinecke N. Laplace-beltrami spectra as 'shape-
664 dna' of surfaces and solids. *Computer-Aided Design* 2006;38(4):342–66.
- 665 [16] Dow M. Integration of calculation models and cad systems in building
666 services design. *Computer-Aided Design* 1987;19(5):226–32.
- 667 [17] Peng F, Guo RS, Li CT, Long M. A semi-fragile watermarking algo-
668 rithm for authenticating 2d cad engineering graphics based on log-polar
669 transformation. *Computer-Aided Design* 2010;42(12):1207–16.
- 670 [18] Marek M, Schreiber I. Chaotic behaviour of deterministic dissipative.
671 Cambridge University Press; 1991.
- 672 [19] Zhang L, Liao X, Wang X. An image encryption approach based on
673 chaotic maps. *Chaos, Solitons and Fractals* 2005;24(3):759–65.
- 674 [20] Mooney A, Keating J, Heffernan D. A detailed study of the generation of
675 optically detectable watermarks using the logistic map. *Chaos, Solitons*
676 *and Fractals* 2006;30(5):1088–97.
- 677 [21] Mooney A, Keating J, Heffernan D. Performance analysis of chaotic
678 and white watermarks in the presence of common watermark attacks.
679 *Chaos, Solitons and Fractals* 2009;42(1):560–70.
- 680 [22] Wang K, Lavoue G, Denis F, Baskurt A. Robust and blind mesh

681 watermarking based on volume moments. *Computers & Graphics*
682 2011;35(1):1–19.

683 [23] Cignoni P, Rocchini C, Scopigno R. Metro: measuring error on simpli-
684 fied surfaces. *Computer Graphics Forum* 1998;17(2):167–74.